RESEARCH ARTICLE

Molecular Nutrition & Food Research
www.mnf-journal.com

Metabolomic Investigation of Brain and Liver in Rats Fed Docosahexaenoic Acid in Regio- and Enantiopure Triacylglycerols

*Raghunath Pariyani, Yumei Zhang, Gudmundur G. Haraldsson, Kang Chen, Kaisa M. Linderborg, and Baoru Yang**

Scope: **N-3 polyunsaturated fatty acids (n-3 PUFAs) play important roles in cognitive functions. However, there is a lack of knowledge on the metabolic impact of regio- and stereo-specific positioning of n-3 PUFAs in dietary triacylglycerols.**

Methods and results: **Rats in a state of mild n-3 PUFA deficiency are fed daily with 360 mg triacylglycerols containing DHA (docosahexaenoic acid) at *sn* (stereospecific numbering)-1, 2, or 3 positions and 18:0 at remaining positions, or an equal amount of tristearin for 5 days. Groups fed with n-3 deficient diet and normal n-3 adequate diet are included as controls. The metabolic profiles of the brain and liver are studied using NMR (nuclear magnetic resonance)-based metabolomics. Several metabolites of significance in membrane integrity and neurotransmission, and glutamate, in particular, are significantly lower in the brain of the groups fed with *sn*-1 and *sn*-3 DHA compared to the *sn*-2 DHA group. Further, the tristearin and DHA groups show a lower lactate level compared to the groups fed on normal or n-3 deficient diet, suggesting a prominent role of C18:0 in regulating energy metabolism.**

Conclusion: **This study sheds light on the impact of stereospecific positioning of DHA in triacylglycerols and the role of dietary stearic acid on metabolism in the brain and liver.**

1. Introduction

Polyunsaturated n-3 fatty acids (n-3 PUFAs) play an important role in human physiology and health. A large body of research has documented the potential significance of PUFAs, especially the role of n-3 PUFAs in reducing the risk of various diseases and metabolic disorders, particularly cardiovascular diseases, neurodegenerative diseases, atherosclerosis, and obesity, among others.[1–3]

Natural sources of n-3 PUFAs in foods are predominantly present in the form of triacylglycerols (TAGs), where the fatty acids are esterified to three stereospecific positions of the glycerol backbone with stereospecific numbering (*sn*) *sn*-1, *sn*-2, and *sn*-3, respectively. The distribution of fatty acids in TAGs of natural fats and oils is not random but under genetic control.[4] For example, unsaturated fatty acids are preferably located at the sn-2 position in most vegetable oils, but mostly in sn-1 and sn-3 positions in animal fats such as lard. On the other hand, saturated fatty acids such as palmitic acid (C16:0) and stearic acid (C18:0) are primarily in sn-1 and rarely in sn-3 in vegetable oils, but in sn-2 in animal fats.[5] Both the composition and the stereospecific location of fatty acids in TAGs influence the digestion, absorption, and metabolic fate of dietary fats and oils.[6]

TAGs are metabolized in a chiral physiological environment. Hydrolysis of TAGs is carried out by lipases, which are typically regioselective. During digestion, fatty acids in the sn-1/3 positions of TAGs are almost completely hydrolyzed by pancreatic lipase, in contrast to only about 22% of fatty acids in the sn-2 position.[7] Further, pancreatic lipases also have a greater affinity for ester bonds in the sn-1 position, compared to those of the sn-3 position.[8] While enantiomers have identical chemical and physical properties, apart from their optical activities, they may have different biological activities in chiral environments like in the human body due to the stereo-specificity/selectivity of the enzymes.[9,10] Several mechanisms contributing to the differences in biological actions of the stereospecifically located fatty acids have been proposed.[8] However, the information available is scanty and inconclusive.

R. Pariyani, K. Chen, K. M. Linderborg, B. Yang
Food Sciences, Department of Life Technologies
University of Turku
Turku 20014, Finland
E-mail: baoru.yang@utu.fi
Y. Zhang
Department of Nutrition & Food Hygiene, School of Public Health
Peking University
Beijing 100191, China
G. G. Haraldsson
Science Institute
University of Iceland
Reykjavik 101, Iceland

The ORCID identification number(s) for the author(s) of this article can be found under https://doi.org/10.1002/mnfr.202300341

DOI: 10.1002/mnfr.202300341

Previously, we reported differential absorption and excretion of DHA from stereospecifically structured TAGs in mildly n-3 PUFA deficient rats.[11] In the current research, we studied the metabolomic profiles of the brain and liver to unravel the possible metabolic pathways involved in the differential metabolic impact of regio- and enantiopure structured TAGs containing DHA and stearic acid. DHA was chosen as it is an n-3 PUFA and an important component of neural membranes, which is present in 30–40% of the phospholipids in the grey matter of the cerebral cortex and photoreceptor cells in the retina.[12] Furthermore, DHA mediates its molecular and cellular effects not only through the regulation of physicochemical properties such as membrane fluidity, permeability, and viscosity in synaptic membranes, but also via modulation of neurotransmission, gene expression, and activities of enzymes, receptors, and ion channels.[13,14]

We hypothesized that NMR-based metabolomics identifies metabolic changes in the brain and liver resulting from differential bioavailability of DHA at different sn-position of TAGs. The brain is one of the major organs having significant needs for DHA for maintaining the integrity and properties of membranes as well as for controlling various neurochemical activities. The brain has low capacity for biosynthesis of DHA. In the absence of dietary DHA, the liver can convert ALA to EPA and DHA as the supply of these fatty acids for the brain. Hence, we chose the brain and liver tissues to study the effect of DHA supplementation in stereospecific locations of TAG mildly n-3 PUFA deficient rats.

In this study, ^{1}H NMR-based metabolomics was used for the untargeted metabolic profiling of the aqueous and nonpolar phases of the tissue extracts prepared from the excised brain and liver of the experimental rats. Pattern recognition combined with other chemometric analyses were applied to identify the metabolites that were potentially influenced by DHA supplementation from different stereospecific positions of TAGs. Based on these findings, the metabolic pathways and networks altered by the intervention are discussed. To the best of our knowledge, this is the first metabolomic study on the effects of DHA using regio- and enantiopure-structured TAGs.

2. Results and Discussion

2.1. Metabolomic Profiling of the Aqueous Extract of the Brain Tissue

Representative ^{1}H NMR spectra of the aqueous extract of the brain tissue extracted from all experimental rats are shown in Figure S2A,B (Supporting Information). As many as to a total of 36 low molecular weight compounds including amino acids, products of glycolysis, intermediates of tricarboxylic acid (TCA) cycle, choline and choline phospholipids, vitamins, and nucleoside derivatives were identified based on their chemical shifts from one- dimensional spectra, and the identities were duly confirmed from 2D NMR spectra. The specific parameters that aided in the identification of metabolites are listed in Table S1, Supporting Information.

A PCA aimed at the comparison of the brain metabolic profile of all rats was performed to explore and visualize the possible clustering trends and detect outliers. The three-dimensional score scatter plot (**Figure 1**) of the PCA showed an apparent clustering of Sn1 and Sn3 groups from other experimental groups. While the three-component PCA model described 85% of the total variance involved in the dataset, the goodness of fit and predictability indicated by $R^2 = 0.934$ and $Q^2 = 0.866$, respectively, endorsed the superior quality of the model. The loading scatter plot indicated the chemical shift regions (hence the identities of metabolites) responsible for the distinct clustering pattern observed in the score plot. Most noticeably, located farther from other metabolite signals, lactate was found to be one of the major discriminatory metabolites.

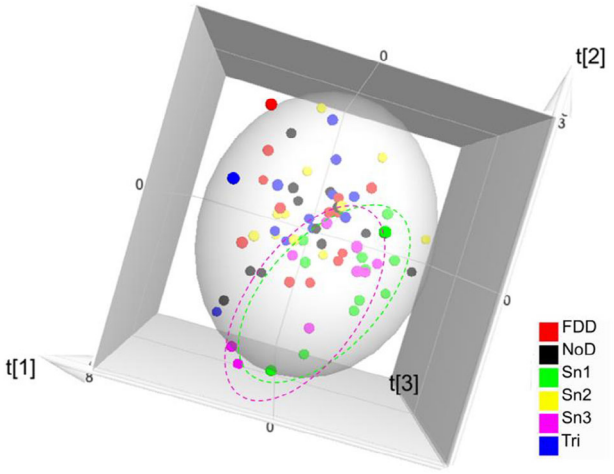

Figure 1. Three-dimensional score scatter plot of a three-component PCA model, with superior goodness-of-fit $R^2 = 0.934$ and predictability $Q^2 = 0.866$, generated from the brain ^{1}H NMR data explained 85% of the total variance in the dataset and discriminated Sn1 and Sn3 groups from other experimental groups. FDD, fatty acid deficient diet; NoD, normal diet; Sn1, Sn2, and Sn3, the groups receiving TAGs with DHA at sn-1, sn-2, and sn-3 position, respectively; Tri, tristearin group.

To further explore the metabolic discrepancies, a pairwise comparison of the experimental groups was performed using supervised OPLS-DA. The parameters goodness-of-fit $R^2X_{(cum)}$, $R^2Y_{(cum)}$, and predictive ability $Q^2Y_{(cum)}$ were used as indicators of the quality of the OPLS-DA models, and details of seven-fold cross-validation and CV-ANOVA used as model diagnostics are tabulated in Table S2, Supporting Information.

As evident from **Figure 2**, OPLS-DA brought about further and clearer separation than that observed in unsupervised PCA. In agreement with the observation from PCA, the Sn1 and Sn3 groups clustered separately from NoD, FDD, and Tri. In addition to that, Tri clustered away from NoD and FDD. Separation was also observed between Sn1 and Sn2 groups. In contrast to Sn1 and Sn3, the Sn2 group did not show separation from NoD, FDD (zero-component models were generated for Sn2 vs NoD and Sn2 vs FDD), or Tri (a statistically nonsignificant model with negative predictive ability was generated).

The metabolites identified based on the correlation coefficient value (Figure 2) and those regions of the spectra contributing significantly to the separation of different models based on the Variable Importance in Projection (VIP $\geq$ 0.8) were considered for quantification using Chenomx NMR Suite Professional 8.6. As many as 17 metabolites among the total of 29 quantified showed statistically significant variation between two or more

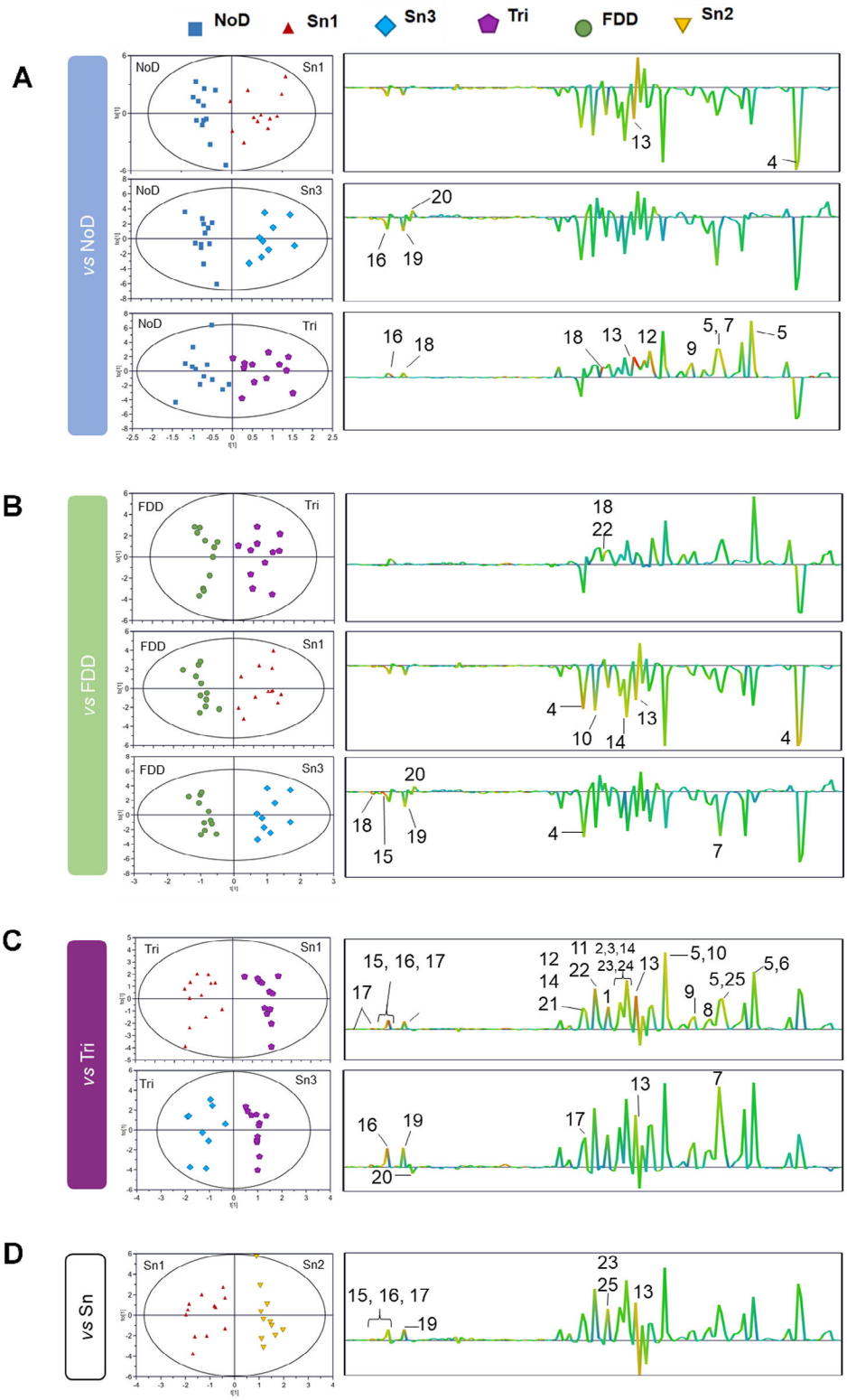

Figure 2. Pairwise supervised OPLS-DA of the brain tissue extracts performed with reference to A) normal diet (NoD), B) fatty acid deficient diet (FDD), C) tristearin (Tri), and D) enantiopure fatty acid (Sn1, Sn2, and Sn3) groups caused the separation of samples (groups) as shown in the score scatter plots and significant discriminatory metabolites in the corresponding color coded coefficient loading plots. Metabolites labeled 1. Leucine; 2. Isoleucine; 3. Valine; 4. Lactate; 5. GABA; 6. Acetate; 7. Glutamate; 8. Succinate; 9. Aspartate; 10. Creatine; 11. Tyrosine; 12. Choline; 13. Taurine; 14. myo-inositol; 15. Inosine; 16. Hypoxanthine; 17. Niacinamide; 18. Unknown; 19. N-acetyl aspartate (NAA); 20. Histidine; 21. O-Phosphocholine; 22. Serine; 23. Glycerol; 24. Glycine; 25. Glutamine.

experimental groups (**Figure 3**). The Tri group showed the highest variation from the Sn1 and Sn3 groups with as many as 16 and 10 metabolites respectively recorded statistically significant differences.

Some amino acids (aspartate, gamma-aminobutyric acid, glutamate, and taurine), choline, lactate, succinate, niacinamide, and hypoxanthine were significantly lower in both Sn1 and Sn3 groups compared to Tri. The Sn1 group particularly showed a significantly lower concentration of some amino acids (isoleucine, leucine, valine, and tyrosine), acetate, creatine, and myo-inositol in comparison with the Tri group.

2.2. Metabolites Derived from Glycolysis and TCA Cycle in Brain

Lactate was found to be the single metabolite involved in causing the separation of all investigated models. Lactate was found at the highest concentration in FDD, while the lowest in the Sn1 group. The brain lactate content in the Sn1 group was statistically lower than the levels in FDD, NoD, and Tri. Also, in the Sn3 group, the lactate level was significantly lower than those in FDD and NoD groups, whereas no statistical difference was observed among the groups FDD, NoD, Tri, and Sn2. The energy production in the brain predominantly takes place through the metabolism of glucose.[15] Glucose can undergo either oxidative metabolism via entering the TCA cycle or produce lactate through anaerobic glycolysis.[16,17] In this study, among all the groups, FDD recorded the highest level of lactate, indicating a pronounced contribution of anaerobic glycolysis and/or a reduction in oxidative metabolism in energy production. Deficiency in n-3 PUFAs may result in glucose hypometabolism via reduced glucose uptake and mitochondrial dysfunction of brain cells leading to impaired brain function, e.g., neurotransmission and neurodegeneration. Elevated lactate has been reported in the brains aging population as well as in Alzheimer's and Parkinson's diseases.[16] Accumulation of lactate in the FDD group fed on n-3 deficient diet could be an indicator of reduced efficiency of the TCA cycle, which could have resulted from impaired function of mitochondria. Dietary supplementation with DHA has been shown to improve the energy metabolism in the brain by increasing the uptake of glucose (via upregulating expression of GLUT1 and GLUT3) and by improving mitochondrial functions.[18,19] This could explain the lower levels of lactate in the Sn1, Sn2, and Sn3 groups fed with DHA in structured TAGs in comparison with other groups.

The β-oxidation of fatty acids serves as an alternate and efficient source of energy in the brain. It has been reported that fatty acid oxidation could contribute up to 20% of the total brain energy requirement in the developing brain.[20] The observation that the FDD had the highest amount of lactate possibly hints at a decrease in the energy production via fatty acid oxidation, compared to other experimental groups, especially the groups receiving structured TAGs having DHA (C22:6) at sn-1 or sn-3 and stearic acid at the remaining positions in the diet.

Compared to the NoD and FDD groups, the Tri (tristearin) group showed a slight reduction (although nonsignificant) in the levels of lactate and a matching increase in the level of succinate. A lower-than-normal lactate concentration may suggest reduced nonoxidative metabolism of glucose, while the elevated levels of succinate along with glutamate—which are major components/indicators of the TCA cycle activity—suggest an increased oxidative metabolism of glucose. In addition to Tri, which has three C18:0 moieties, reduction in the lactate levels was also observed in all the DHA groups, which possess two C18:0 moieties. These findings taken together are in line with previous findings showing that C18:0 consumption caused an upregulation of the β-oxidation of fatty acids in humans as suggested by the reduction in the circulating acylcarnitine levels.[21]

2.3. Effects on Amino Acids and Neurotransmitters in the Brain

Amino acids were among the key metabolites in differentiating the groups fed on a different diets (Figure 3). Compared to other groups, the Tri group was characterized by a higher content of three branched-chain amino acids (BCAA), valine, leucine, and isoleucine, the difference reaching statistical significance in comparison to the Sn1 group. Similar differences were found in the content of some other amino acids including glutamate, GABA, taurine, and tyrosine, recording significant differences compared to Sn1 and Sn3 groups.

The brain is a major organ for metabolizing BCAA. As essential amino acids BCAA is required for the biosynthesis of proteins. Leucine acts as an anabolic nutrient signal activating mTOR, a serine/threonine protein kinase, which is involved in regulating protein and lipid biosynthesis as well as cell proliferation and growth.[22] Dietary intervention with leucine regulates hypothalamic mTORC1 signaling and results in the suppression of food intake.[22] BCAA also acts as nitrogen donors for the biosynthesis of glutamate and glutamine.[23] Glutamate is an excitatory neurotransmitter and a crucial link between amino acid and glucose metabolism through the TCA cycle. Glutamate level in the brain showed a statistically significant increase in the Sn2 compared to the Sn1 and Sn3 groups. The glutamate level was also higher in the Tri group than in the Sn1 and Sn3 groups.

Increased content of BCAA and enhanced activation of BCAA metabolism-associated enzymes in the hippocampus of the brain was found to be strongly associated with the high learning ability phenotype in Tokai high avoider (THA) rats in comparison with the parental Wistar rat strain.[23] The BCAA content was found to be reduced in the brain of patients with Alzheimer's disease (AD), and a lower level of valine in plasma was shown to be associated with an increased risk of dementia and AD as discussed in a recent review.[16] However, it is worth noticing that both excessive levels of BCAA as a result of impaired metabolism of BCAA and depletion of BCAA by uncontrolled BCAA catabolism lead to neurological consequences. Therefore, further study is needed to establish the physiological impact of the increased BCAA level in the brain of the Tri group.

As a major amino acid in the brain, taurine is involved in multiple biochemical and physiological processes in the brain including neurotransmission, maintaining osmolarity, regulating insulin response and antioxidative status, and stabilizing mitochondria. Taurine stabilizes membranes through direct interactions with phospholipids. Taurine deficiency leads to a delay in cell differentiation and migration in the cerebellum, pyramidal cells, and visual cortex in animals.[24]

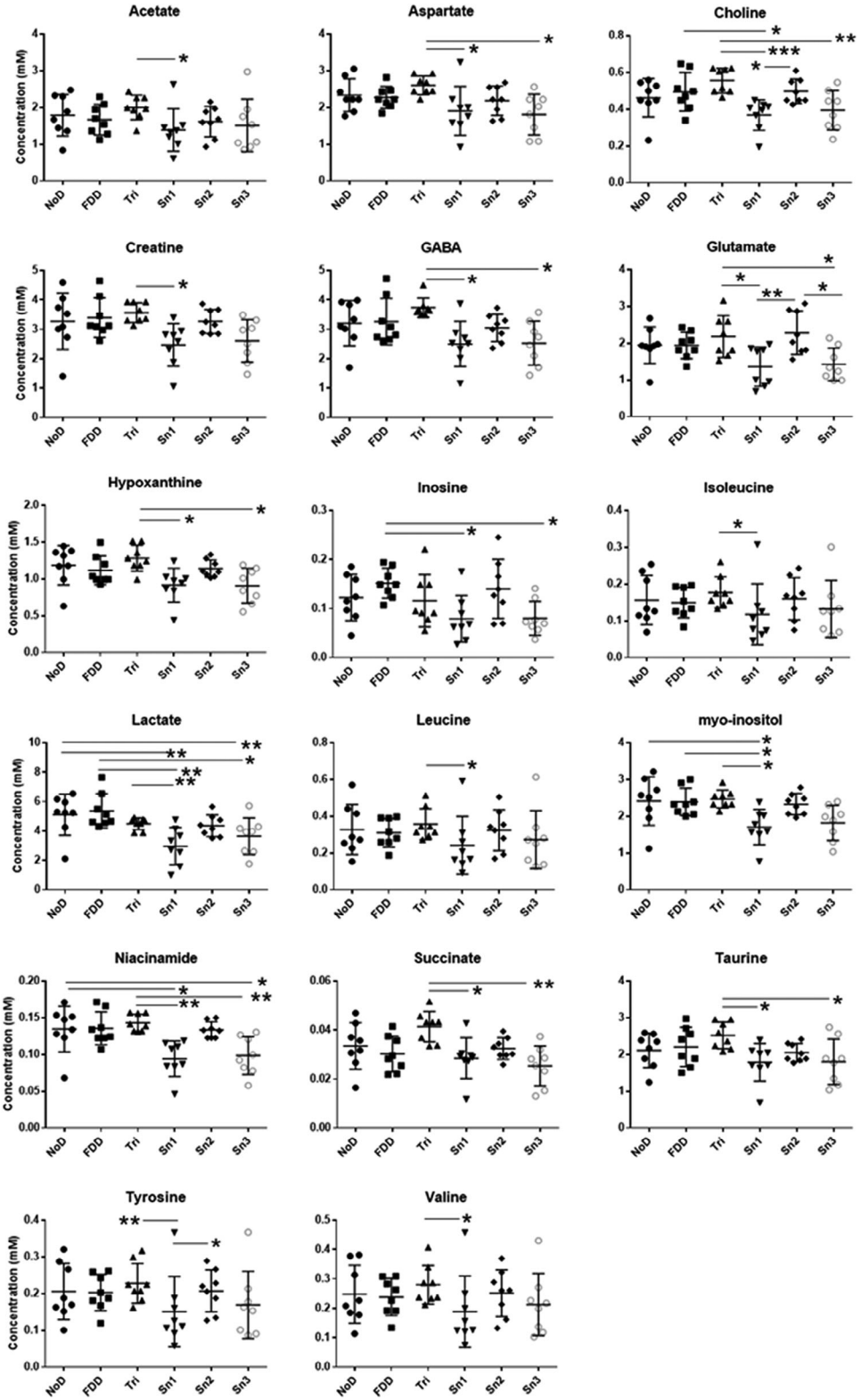

Figure 3. Scatter plots of metabolites quantified from ^{1}H NMR spectra of the brain tissue extract. The horizontal lines represent the mean, and the vertical lines represent SD. Statistical significance was identified via One-way ANOVA coupled with posthoc tests. Levels of statistical significance are as follows: $*p < 0.05$; $**p < 0.01$; $***p < 0.001$. Metabolites were quantified using Chenomx NMR Suite Professional 8.6, with reference to the methyl signal of DSS-d6 at 0 ppm.

Taurine is considered a neuroprotective amino acid.[25,26] Research evidence suggests that taurine may improve neuronal function in subjects with obesity and diabetes through various mechanisms such as modulating inhibitory neurotransmission, stimulating antioxidant systems, and influencing Ca^{2+} homeostasis.[26]

The Tri group showed a significantly higher content of taurine in the brain indicating a potential role of stearic acid in regulating taurine homeostasis in the brain in rats. Previously, an in vitro study showed that stearic acid dose-dependently protected rat brain slices against toxicity induced by oxygen-glucose deprivation and glutamate as well as from damage caused by oxidative stress. The neuroprotective effect of stearic acid was possibly mediated by the activation of PPAR-γ, phosphatidylinositol 3-kinase dependent mechanism, and by boosting the internal antioxidant enzymes in brain tissue.[27] The relevance of the findings of this study and previous research on the potential effects of stearic acid on brain in the context of human nutrition remains to be investigated.

Glutamate is an excitatory neurotransmitter whose biological effects are altered/modulated by GABA (gamma-aminobutyric acid), which is a major inhibitory neurotransmitter present in the cerebral cortex. Glutamate is the precursor for the synthesis of GABA. An impaired glutamate/GABA-glutamine cycle has been linked to aging as well as many neurochemical disorders such as AD, autism spectrum disorder, schizophrenia, traumatic brain injury, and stroke.[28] The patterns of distribution of glutamate and GABA as shown in Figure 3 indicate a perturbation in neurotransmitter recycling/production and a possible internal compensatory mechanism to balance the excitatory and inhibitory effects exerted by the neurotransmitters glutamate and GABA, respectively.

It has been shown earlier that DHA increases glutamatergic activity in the brain through multiple mechanisms. DHA enhances glutamatergic synaptic activities with concomitant increases in synapse and glutamate receptor subunit expression in hippocampal neurons.[29] Spontaneous synaptic activity is significantly increased due to enhanced glutamatergic activity in DHA-supplemented neurons. On the other hand, lack of DHA results in inhibition of synaptogenesis, decrease in synapsins and glutamate receptor subunits, and impairment of long-term potentiation in hippocampal neurons. In addition, DHA stimulates the activities of glutamate transporters (GLT1, GLAST, and EAAC1).[30]

In contrast to enhanced glutamatergic activity, DHA inhibits GABA receptor-mediated responses in cultured neural cells in a concentration and time-dependent manner.[31] It is suggested that the effect of DHA on the GABA receptor is due to the effect on the lipid microenvironment for the GABA receptors.[12] However, the GABA levels did not show a statistically significant difference among the groups receiving DHA in regio- and enantiopure TAGs. Nevertheless, the pattern of compensatory change reflecting the glutamate concentration was evident in the GABA levels.

2.4. Metabolites Affecting Membrane Integrity

Choline is a donor of methyl group in methionine metabolism and an essential component of phospholipids contributing to the structural integrity of cell membranes. Furthermore, choline has a critical role in neurotransmission primarily because of its role in the synthesis of acetylcholine as well as its modulatory effects on the dopaminergic system. Abnormal choline transport and metabolism have been implicated in a number of neurodegenerative disorders such as AD and Parkinson's disease. The ability of unsaturated fatty acids, DHA in particular, to enhance the choline uptake and transport systems has been demonstrated in various in vivo and in vitro studies.[32,33] The Sn1/3 groups had a lower level of choline in the brain compared to the Sn2 and Tri groups. Thus, this finding hint that the DHA at *sn*-1/3 positions but not *sn*-2 position of TAG affected choline transport/metabolism, which might be related to the higher absorption rate of 18:0 from *sn*-2 compared to *sn*-1 and *sn*-3 positions. However, the mechanism needs to be further investigated.

A trend similar to that observed with choline was evident in myo-inositol as well. In the animal brain and muscle tissues, myo-inositol is a principal product of phosphatidylinositol (PI) hydrolysis as well as a precursor for PI synthesis. It mediates cell signal transduction in response to a variety of hormones, neurotransmitters, and growth factors and participates in osmoregulation. Perinatal n-3 PUFA (alpha linolenic acid) deficiency resulted in decrease in DHA level in the prefrontal cortex, which correlated with reduced myo-inositol concentrations and augment receptor-generated myo-inositol synthesis in rats.[34] In a human intervention and follow-up study, supplementation with long-chain polyunsaturated fatty acids including DHA during infancy increased the concentration of myo-inositol in the brain at the age of 9 years.[35] However, we did not see a decreased level in the n-3 PUFA deficient groups (FDD and Tri) compared to the n-3 PUFA adequate group (NoD).

2.5. Metabolic Pathway Analysis of the Brain

The quantitative metabolic pathway analysis integrating pathway enrichment analysis and pathway topology analysis aids in the consistent and systematic identification of statistically significant pathways altered as a result of an intervention by extracting the information on the discrete metabolite/biomarker concentrations. In order to perform metabolic pathway analysis, the six experimental groups were regrouped and reduced to three groups based on the observations from multivariate data analysis and quantification data of the metabolites. The NoD and Sn2 sharing similar metabolic trends were included in group 1, while Sn1 and Sn3 constituted group 2, and the tristearin group (Tri) was considered the third group. When groups 1 and 2 were subjected to metabolic pathway analysis, among the several metabolic pathways shown to have been affected, two were identified to be statistically significantly altered based on the set criteria of Holm *p*-value (adjusted by Holm–Bonferroni method) and false discovery rate (FDR)- adjusted *p* values lower than 0.05, and the impact score (indicating the impact of significantly affected metabolites in the pathway based on network topology measure of relative betweenness centrality) higher than 0.4. From **Figure** 4A it could be observed that the glutamine and glutamate metabolism and alanine, aspartate, and glutamate metabolism were the significantly affected pathways. In the next step, the FDD group, which showed closely similar metabolic

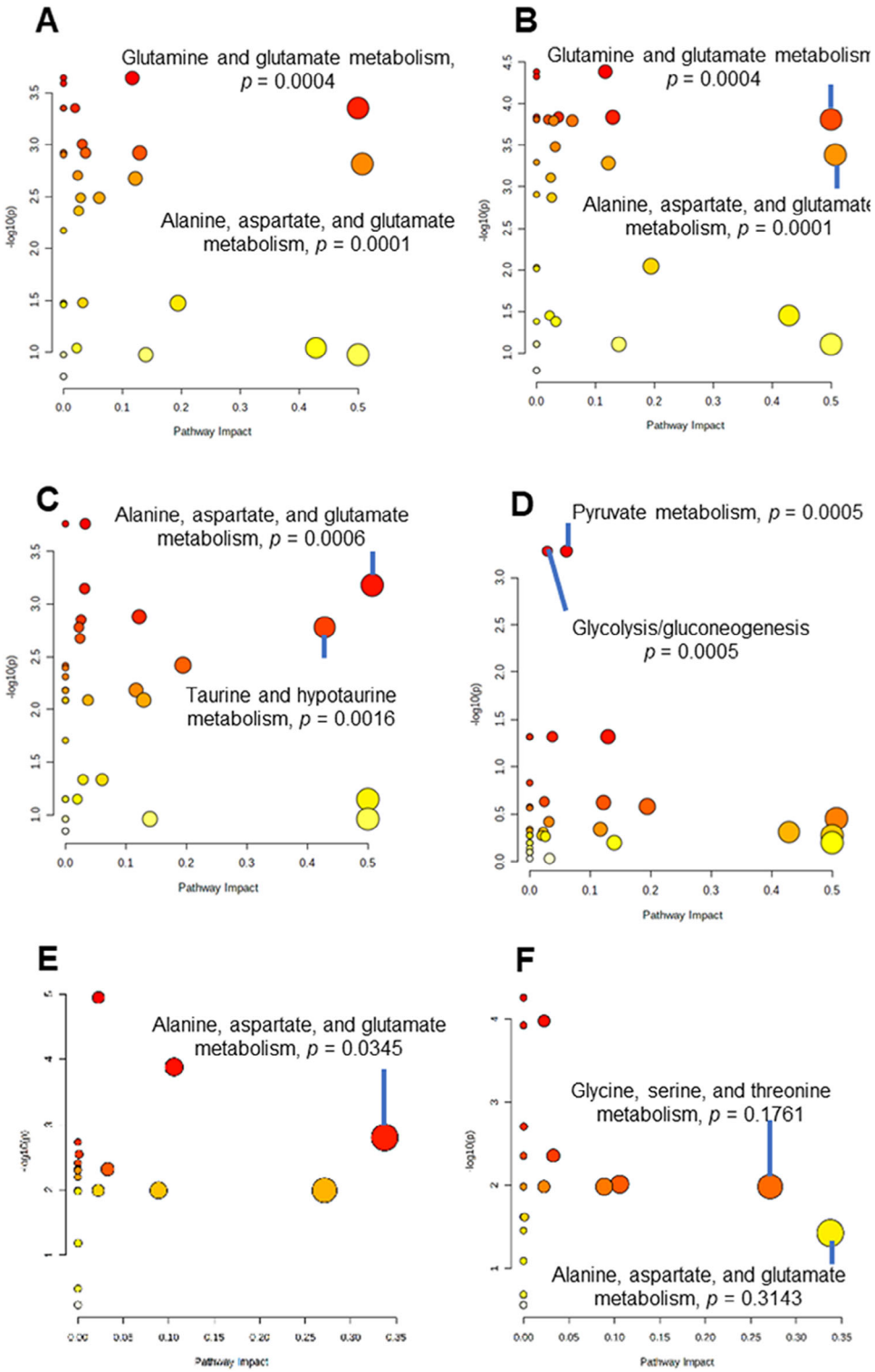

Figure 4. Major metabolic pathways altered by different experimental fatty acid diets as identified from the ^{1}H NMR metabolomics. Brain – A) NoD+Sn2 versus Sn1+Sn3; B) FDD+NoD+Sn2 versus Sn1+Sn3; C) Tri versus Snx; D) FDD+NoD versus Tri+Snx; Liver; E) NoD versus Tri; F) NoD versus Snx. This was achieved by pathway analysis integrating pathway enrichment analysis and pathway topology analysis using MetaboAnalyst 5.0, which is an open-source web-based metabolomics data analysis platform.

properties to NoD, was also added to group 1 and the metabolic pathway analysis was repeated with group 2. As expected, the significantly affected metabolic pathways remained the same (Figure 4B) as in the original analysis of group 1 versus 2.

In the third analysis model, the tristearin group (Tri) was compared with the DHA groups, alanine, aspartate, and glutamate metabolic pathway was identified to be significantly altered (Figure 4C). In addition, another metabolic pathway related to energy metabolism, i.e., taurine and hypotaurine metabolism, was also found to be significantly affected, but with a slightly lesser, yet significant, pathway impact value of 0.4. This upregulation in the energy metabolism, predictably, caused by Tri (C18:0) was evident by the elevated amounts of taurine in quantification data. In a separate model, when the groups fed with DHA-containing TAGs or tristearin were subjected to metabolic pathway analysis with FDD and NoD groups, pyruvate metabolism, and glycolysis/gluconeogenesis were found to be significantly influenced based on the Holm *p*-value e FDR-adjusted *p*-values, however, the pathway impact was negligible (below 0.08) (Figure 4D).

Thus, the most significantly affected pathway among all the analyzed models was related to amino acid metabolism, i.e., alanine, aspartate, and glutamate metabolism. Among the metabolites, glutamate was identified to be the one single altered metabolite having a significant influence on amino acid metabolism as well as neurotransmission (via glutamine and glutamate metabolism).

2.6. Metabolomic Profiling of the Aqueous Phase of the Liver Tissue Extracts

Representative ^{1}H NMR spectra of the aqueous extract of the liver tissue extracted from all experimental groups are shown in Figure S2C,D (Supporting Information). Based on the chemical shift from 1D ^{1}H NMR spectra and correlations from 2D NMR spectra, a total of 51 metabolites including amino acids, amino acid derived metabolites, TCA cycle intermediates, choline and choline phospholipids, vitamins, and nucleoside derivatives were identified, as listed in Table S1, Supporting Information.

The score plot of a two-component PCA model with satisfactory goodness-of-fit $R^2 = 0.742$ and predictability $Q^2 = 0.7$ displayed a trend in the clustering of samples (**Figure 5**A). A distinct metabolic profile of NoD was strikingly evident as most of the NoD samples were seen on the first quadrant of the score plot, separated from the rest of the samples by PC1. FDD samples in general were located between NoD and that of a cluster formed by samples from the DHA groups as well as Tri seen distributed in quadrants 2, 3, and 4. Most of the samples from the Sn3 group showed a pattern of clustering along the negative axis of PC2.

Pairwise comparison of all experimental groups using OPLS-DA models reinforced the distinct metabolic profile of NoD compared to other groups, especially Tri and the DHA groups. Four models, namely, NoD versus Tri, Sn1, Sn2, and Sn3, respectively, were statistically significant in causing a separation between the compared groups (Figure 5B). Other models generated were either nonsignificant or overfit as proved by the validation tools. The goodness-of-fit $R^2X_{(cum)}$, $R^2Y_{(cum)}$, and predictive ability $Q^2Y_{(cum)}$ of the OPLS-DA models, and details of seven-fold cross-validation and CV-ANOVA used as model diagnostics are tabulated in Table S3, Supporting Information.

The color-coded coefficient loading plots shown in Figure 5B is labeled with metabolites having a correlation coefficient ≥0.7. The metabolites identified based on the correlation coefficient value and those regions of the spectra contributing significantly to the separation of different models based on the Variable Importance in Projection (VIP ≥ 0.8) were considered for quantification using Chenomx NMR Suite Professional 8.6. Eleven metabolites among the total of 30 included in quantification showed statistically significant variation between different groups (**Figure 6**).

3-Hydroxybutyrate and O-phosphocholine were found in elevated concentrations in all DHA-supplemented groups compared to NoD. Ketone bodies—3-hydroxybutyrate (3-HBT), acetoacetate, and acetone, are predominately produced in the liver as a product of the normal metabolism of fatty acid oxidation, which serves as an important energy source during energy restriction or in the absence of sufficient blood glucose. O-phosphocholine, an intermediate in the synthesis of phosphatidylcholine, was identified as a common dysregulated metabolite in gluco-, lipo-, and glucolipo-toxic conditions with significantly reduced levels.[36] Two other major metabolites that showed significant differences were adenosine and glutamine, at their lowest and highest concentrations, respectively, in the Tri group.

Among the metabolic pathway analysis performed between different experimental groups, two separate sets of analysis showed alteration in some of the metabolic pathways. In the first case, the NoD group was compared with Tri, where three metabolites, namely aspartate, glutamine, and succinate caused a significant change in the alanine, aspartate, and glutamate metabolic pathways (Holm *p*-value 0.03, FDR adjusted *p*-value 0.01) (Figure 4E). This pathway was consistently identified as the most perturbed in the brain samples as well, when comparing NOD/Sn2 versus Sn1/Sn3 and Tri versus the DHA groups. However, unlike the brain samples where the pathway impact was above 0.5, in the case of the liver samples, it had a lesser impact recorded at 0.3. This was in line with the pattern of distribution evident from the quantification data. Secondly, NoD was compared with the groups supplemented with DHA (Figure 4F). Although two pathways, namely glycine, serine, and threonine metabolism and alanine, aspartate, and glutamate metabolism had an impact value of 0.28 (Holm *p* 0.17, FDR 0.02) and 0.33 (Holm *p* 0.31, FDR 0.05), respectively, none of these proved to be significant by the criteria of 0.05 for Holm and FDR adjusted *p*-value. Thus, as a summary, the one pathway that was altered in both brain and liver samples was alanine, aspartate, and glutamate metabolism.

2.7. Normal Versus n-3 Deficient Diet

The impact of dietary intake of n-3 PUFAs and n-3 PUFA deficiency on DHA levels in various tissues has been widely investigated. However, the subsequent effect of these changes on the metabolic profile has not been systematically investigated yet. Previously, we observed significant decreases in the DHA content in the liver (by 14%) and brain (by 50%) of the FDD group compared to the NoD group.[37] In this study, a comparison of the metabolomic profiles of the liver and brain tissues of the NoD and

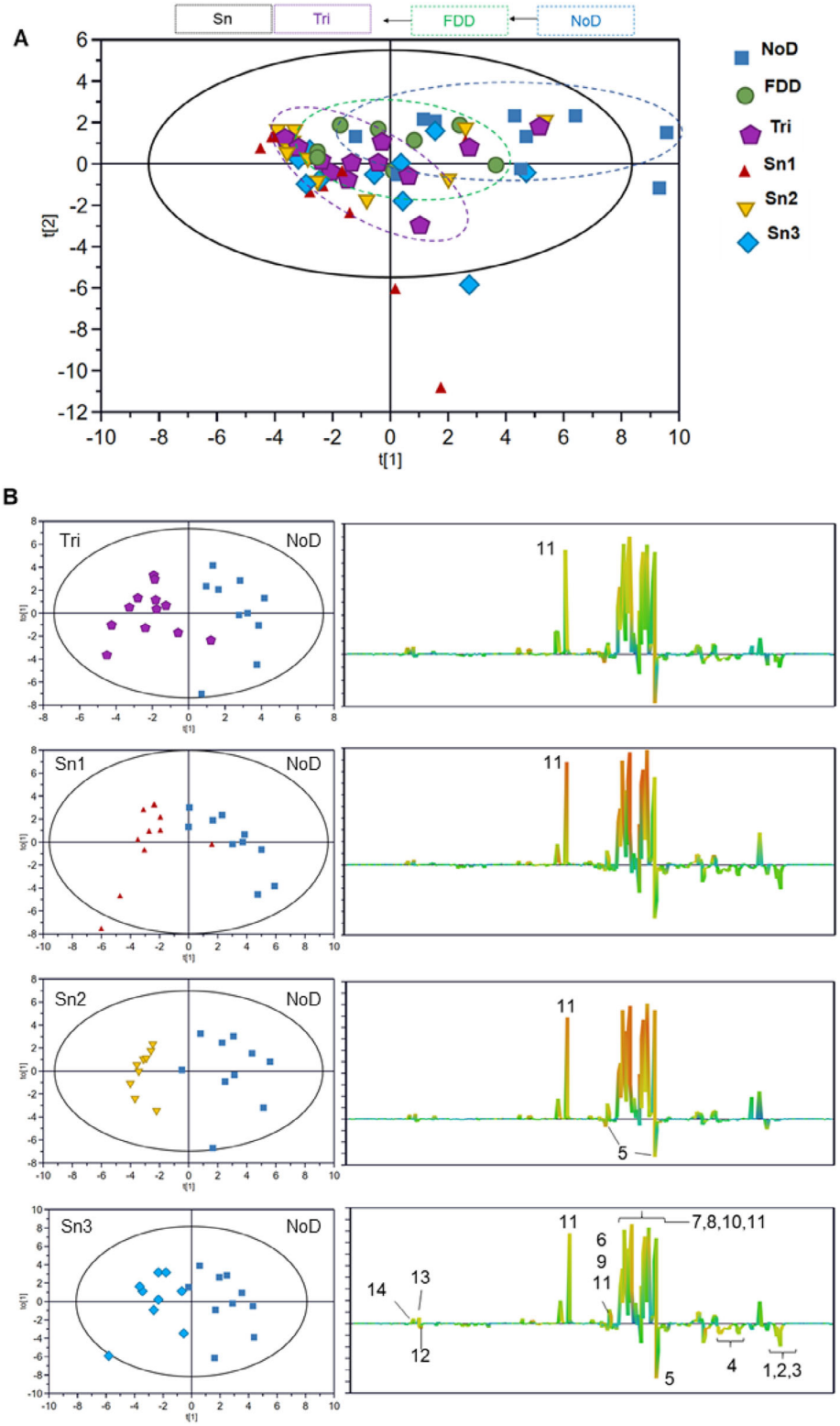

Figure 5. A) Score scatter plot of a two-component PCA model with satisfactory goodness-of-fit $R^2 = 0.742$ and predictability $Q^2 = 0.7$, generated from the liver tissue extract ^{1}H NMR data, explained 74% of the total variance in the dataset. A pattern of distribution of the experimental groups was evident in which NoD was clearly separated from others. B) Pairwise OPLS-DA models generated in comparison with NoD showed distinct clustering in the score plots and the corresponding color-coded coefficient loading plots identified significant discriminatory metabolites. Metabolites labeled 1. Leucine; 2. Isoleucine; 3. Valine; 4. Glutamate; 5. O-Phosphocholine; 6. Glycerol; 7. Betaine; 8. Aspartate; 9. Serine; 10. Lactate; 11. Glucose; 12. Niacinamide; 13. Hypoxanthine; 14. Adenosine. FDD-fatty acid deficient diet; NoD-normal diet; Snx-enantiopure fatty acid group(s); Tri-tristearin group.

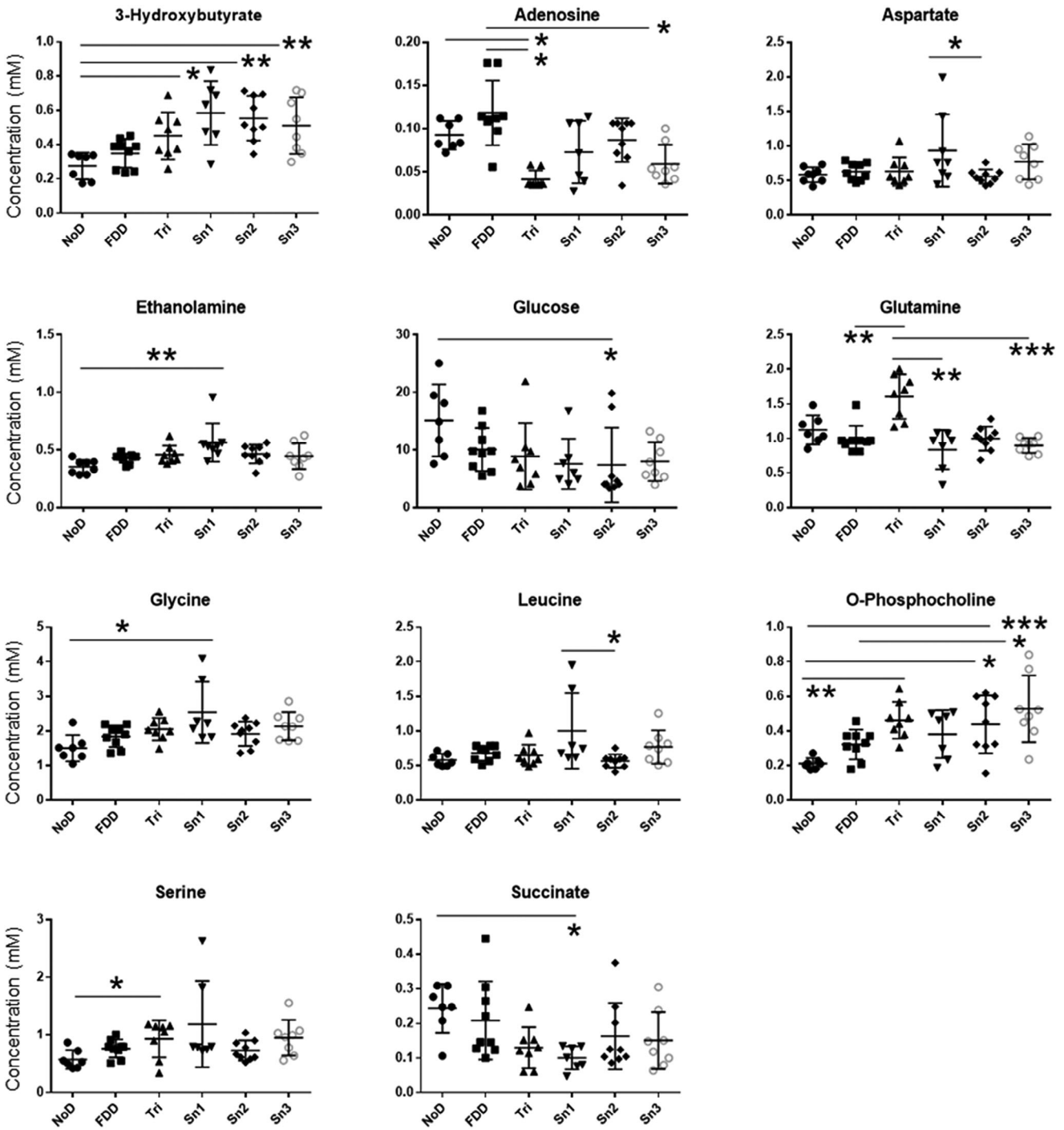

Figure 6. Scatter plots of metabolites quantified from the ^{1}H NMR spectra of the liver tissue extract. The horizontal lines represent the mean, and the vertical lines represent SD. Statistical significance was identified via One-way ANOVA coupled with posthoc tests. Levels of statistical significance are as follows: *$p < 0.05$; **$p < 0.01$; ***$p < 0.001$. Metabolites were quantified using Chenomx NMR Suite Professional 8.6, with reference to the methyl signal of DSS-d6 at 0 ppm.

FDD groups did not show any statistically significant difference either in multivariate or univariate analysis.

It is also worth noting that the deficiency state induced in this study was mild first-generation deficiency. Compared to plasma, the lipid profile and metabolism in brain is more buffered against changes in dietary intake of n-3 PUFAs,[38] possibly due to some internal compensatory mechanisms upon sensing a deficiency in n-3 PUFAs. When rats were subjected to 15-week deprivation of dietary n-3 PUFA, the reduction in brain DHA concentration was accompanied by a prolonged brain DHA half-life.[39]

Furthermore, the activities of presumably DHA-selective iPLA2, acyl-CoA acyltransferases, and COX-1 were found to be reduced. These are the enzymes/messengers involved in the turnover of DHA through deacylation-reacylation and oxidation mechanisms.

An acute (2-week) dietary supplementation of DHA showed that there was a greater overall responsiveness as changes of DHA level in plasma compared to the brain, which may reflect a more circumscribed homeostatic response range of brain lipids to dietary DHA supplementation.[38] Another consistent biochemical compensatory measure occurring in the brain during a reduced brain phospholipid DHA is popularly known as "homeoviscous compensation,"[40] describing the reciprocal increase in long-chain n-6 PUFA, especially arachidonic acid, in response to a reduction in n-3 DHA.

These changes as a whole serve as a mechanism to maintain the degree of unsaturation of cell membranes and to minimize the metabolic perturbations. In agreement with the previous findings, the lipidomic analysis of the samples from our feeding trial indeed revealed a compensatory increase of arachidonic acid (20:4n-6) in the brain of FDD group compared to the NoD and DHA supplemented groups.[37] This further hints that the time window for the induction of significant metabolic changes, particularly those related to growth and maintenance, may be longer than the 5 weeks involved in the current study.

2.8. Comparison of Regio- and Enantio-Structured TAGs Containing DHA at Different Stereospecfic Positions

Generally, it is widely accepted that the n-3 PUFAs located in the sn-2 position are more efficiently absorbed compared to the n-3 PUFAs located in the sn-1/3 positions.[41,42] During fat digestion, pancreatic lipase hydrolyses dietary TAGs releasing free fatty acids from the sn-1 and sn-3 positions and resulting in sn-2-monoacylglcyerols. After digestion, long chain free fatty acids are absorbed via a protein-mediated process, whereas monoacylglycerols are absorbed through passive diffusion. The structural features of fatty acids, e.g., carbon chain length and degree of unsaturation, also influence the absorption efficiency of free fatty acids due to different tendency to the form insoluble calcium soap and varying affinity of fatty acid transport proteins.[8] Although the lipidomic analysis of the fecal samples from the rats of this experiment indicated a slightly superior absorption of DHA from the sn-2 position compared with sn-1 and sn-3 positions,[11] no statistically significant differences were found in the levels of DHA in the fasting plasma, liver, or brain among these groups, which indicated overall similarity in bioavailability of DHA among the three DHA groups.[11,37] In both liver and brain samples, the metabolic profile of the Sn1 and Sn3 groups was almost similar, however, they showed a slightly different trend compared to Sn2. Nevertheless, glutamate and choline were the only metabolites in the brain to show statistically significant difference among the Sn1, Sn2, and Sn3 groups. The level of glutamate in the brain was higher in Sn2 group than in Sn1 and Sn3 groups, whereas that of choline was higher in Sn2 group compared to the Sn1 group. In addition to the different stereospecific position of DHA, the differential absorption of stearic acid from different sn-positions of TAGs could have contributed to the metabolic impact.

2.9. Differential Metabolic Impact between Tristearin and Regio- and Enantiopure TAGs Containing DHA and Stearic Acid

The rats in the tristearin group and the DHA groups all received stearic acid in the diet during the 5-day test feeding. Contrary to the general observation that saturated fatty acids are harmful, dietary stearic acid has been reported to possess neutral to beneficial effects on various physiological conditions, including cardiovascular system disorders. Increased levels of circulating C18:0 lipids are associated with reduced blood pressure, improved heart function, and reduced cancer risk.[43,44]

Despite similar levels of C18:0 in fasting plasma,[11] the Tri group recorded a significantly higher fecal loss of C18:0 compared to the DHA groups. The metabolic profile of the Tri group in both brain and liver samples was marked with a characteristic pattern of changes in some of the metabolites in comparison with other experimental groups, particularly those related to energy metabolism. Among the metabolites found upregulated in the Tri group, choline, taurine, succinate, and GABA deserve special attention. All these metabolites were present in their highest quantities in the Tri group, whereas a statistically markedly lower levels were observed in the Sn1 and Sn3 groups. The Sn2 group had either almost similar or a little reduced (statistically nonsignificant) levels of these metabolites compared to the Tri and NoD.

DHA levels in plasma, brain, and liver showed a significant reduction in the Tri group in comparison with the DHA groups.[11] Withstanding this obvious difference in DHA levels, the metabolic profiles of Tri and Sn2 were similar in this study, suggesting the absence of direct link connecting the levels of DHA with the metabolic responses.

2.10. Metabolomic Analysis of the NMR Spectra of the Non-Polar Phase of Brain and Liver Tissue Extracts

NMR spectra of the nonpolar phase of the brain and liver tissue extracts have shown signals characteristic of cholesterol, fatty acids, glycerophospholipids, choline, phosphatidylcholine, and sphingomyelin among others (Figure S5A,B, Supporting Information). Chemometric analysis employing PCA on the NMR spectra of the nonpolar phase of the brain extracts did not show clear discrimination of the groups receiving different diets (Figure S5C1, Supporting Information). However, a mild trend of distribution of samples belonging to the Sn3 group could be proposed as having a slightly distinct clustering pattern compared to the spectra of other samples. However, the model diagnostics were poor for the two-component PCA model, which recorded an R2 of 0.509 and Q2 of 0.361, suggesting lower-than-optimum goodness of fit and low predictive ability. Nevertheless, a PLS-DA was performed to see if a clearer separation of Sn3 could be achieved (Figure S5C2, Supporting Information). Nonetheless, a two-component model with R2 (cum) 0.469, R2Y (cum) 0.181, and Q2 cum 0.0761 denoted the model to be of inferior quality. The model was further rejected by 100 permutation tests

by qualifying the necessary criteria for proving to overfit (Figure S5C3, Supporting Information). Altogether, it implied that the metabolite variations, as determined by NMR spectroscopy, in the nonpolar phase of the spectra of brain extracts from different experimental groups were insignificant.

Similarly, chemometric analysis of the NMR spectra of the nonpolar phase of the liver extracts did not show a difference among the groups. A two-component PCA model with superior goodness of fit (R2 = 0.959) and predictive ability (Q2 = 0.915) showed that the majority of the samples were grouped together at the center of the score scatter plot (Figure S5C4, Supporting Information). Among other observations, the presence of two critical outliers was also noted. Hence, a separate PCA model was constructed by excluding the two outliers to remove their possible influence on the distribution pattern of the remaining samples. However, the observation from the score plot (Figure S5C5, Supporting Information) was similar to the earlier one, lacking any distinct clustering trends. Therefore, the nonpolar phases of neither the brain nor the liver extracts were discriminated against based on the diet by NMR spectroscopy coupled with chemometric analysis.

3. Concluding Remarks

The metabolism and bioavailability of dietary PUFAs have been suggested to be influenced by their stereospecific locations in TAGs. Herein, regio- and enantiopure structured TAGs containing DHA either in sn-1, sn-2, or sn-3 positions and stearic acid in the remaining positions were fed to rats, and the metabolic effects on the brain and liver were studied using NMR spectroscopy-based metabolomics. Higher content of glutamate in the brain clearly distinguished the rats fed on sn-2 DHA from those on DHA in sn-1 and sn-3 positions of TAGs. Many metabolites related to energy metabolism and neurotransmission were significantly lower in the brain tissue of sn-1 and sn-3 DHA groups compared to the tristearin group, indicating the possible influence by both DHA and stearic acid in the diet. Significantly affected pathways included glutamine and glutamate metabolism and alanine, aspartate, and glutamate metabolism. Meanwhile, the brains of rats maintained on a tristearin diet showed distinctly higher levels of taurine and succinate compared to other groups, metabolites related to energy metabolism. While in the liver tissues, ketone bodies, such as 3-HBT, linked to energy metabolism were seen elevated in the groups fed with DHA. Thus, the metabolomics approach differentiated the effects of feed supplementation with structured TAGs containing DHA and stearic acids in the regulation of various metabolic pathways and thus provided new insights for a better understanding of their molecular mechanism. To the best of our knowledge, this is the first comprehensive metabolomic analysis to identify the effects of regio- and enantiopure-structured TAGs, particularly through a nutritional study comprised of several feeding days. Feeding on n-3 deficient diet for 5 weeks did not result in significant changes in the metabolomic profile in the brain and liver in rats compared to those received normal diet. This reinforced the theory of internal compensatory mechanism in operation possibly via varying the enzymes involved in metabolism and/or extending the half-life of DHA to maintain homeostasis.

4. Experimental Section

Synthesis of Regio- and Enantiopure Structured TAGs: A two-step chemoenzymatic process using glycerol and a highly regioselective immobilized Candida antarctica lipase (CAL-B) was used in the synthesis of TAG possessing DHA in the sn-2 position and stearic acid in the sn-1 and 3 positions.[45] The chemical and regioisomeric purity (>98%) was confirmed using ^{1}H (400 MHz) and ^{13}C NMR, IR spectroscopy, and mass spectrometry analyses.[9]

Intervention Feeding: The protocol of the animal experiment was approved by the Medical Ethics Research Board of the Peking University Health Science Center, China (LA2016043).

Briefly, a total of 72 male Sprague–Dawley rats (age 21 ± 2 days) were kept for 1 week in isolation with constant temperature and humidity and on adaptive feeding of standard AIN-93G diet which contained soybean oil as a source of n-3 FA. After a week of acclimatization, the rats were randomly divided into 6 experimental groups of 12 animals each. Five groups were fed with modified AIN-93G containing n-3 FA deficient peanut oil as the only source of FAs for 4 weeks to induce a mild n-3 FA deficient state, while the sixth group was fed on the standard AIN-93G containing soybean oil (NoD). The feeding of animals and feed composition was reported in details in the previously published papers.[11,37]

Following the induction phase of 4 weeks, four of the n-3 deficient groups received daily 360 mg of 2,3-distearoyl-1-docosahexaenoyl-sn-glycerol (Sn1), 1,3-distearoyl-2-docosahexaenoyl-sn-glycerol (Sn2), 1,2-distearoyl-3-docosahexaenoyl-sn-glycerol (Sn3), or tristearin (Tri) as the experimental fat for 5 days (the intervention phase), whereas the fifth group continued modified AIN-93G to receive the n-3 FA deficient peanut oil (FDD) with the composition described in Kulkarni et al.[37] The normal diet group (NoD) continued the standard AIN-93G diet from the beginning till the end of the experiment. A diagrammatic presentation of the experimental design was shown in Figure S1, Supporting Information. At the end of the intervention phase (on day 6), the rats were sacrificed, and the organs including the brain and the liver were collected from each rat, weighed, and immediately frozen and stored at −80 °C until analysis. The details of the study design, the composition of the diet in different groups, housing and maintenance, feed and water intake, sample collection methods, and the weight of organs and the body were also reported earlier.[11]

Dosage Information: Each rat was given a daily dosage of 360 mg of experimental fat embedded between two halves of a low n-3 FA feed pellet, which served as the first morning feed. Once verified that the experimental fat pellets were consumed completely, the rats were provided with free access of feed and water. The dose was chosen based on previously review and study both in humans and rat.[46,47] According to human equivalent dose calculation method,[48] human equivalent dose was 23.5 g for a 60 kg adult, which was rational.

Sample Preparation for NMR Spectroscopy: On removal from the −80 °C freezer, the brain and liver tissues were allowed to thaw on ice. Small pieces cut at random using a surgical blade from both external and internal regions of the whole tissue were weighed out to a preweighed ice-cold glass vial to get a final cumulative sample weight of around 250 mg (250 ± 28 mg, mean ± SD). The extraction of metabolites was performed according to a published protocol[49] with slight modifications. Briefly, 2.0 mL cold methanol and 0.425 mL ultrapure cold water were added to the tissue sample in the glass vial and vortexed for 1 min. It was homogenized using an ultraturrax (IKA 25) for 1 min divided into three sessions of 20 s duration each. Then, 2 mL of ice-cold chloroform and 1 mL of ultrapure cold water were added, and the mixture was vortexed for 1 min. The samples were allowed to rest on ice for 1 h. Centrifugation of the sample vials for 15 min at 1500 × *g* and 4 °C caused the separation of lower nonpolar and upper polar (methanol/water) phases. The upper phase was collected, and the solvents were removed by lyophilization. The yield of the dried phase was recorded, and the dried residue was then reconstituted using NMR solvent comprised of 80% water and 20% Chenomx internal standard solution-IS2, adjusted to pH 7.4 with KH_2PO_4 buffer. The Chenomx internal standard solution IS-2 consisted of deuterated DSS (DSS-d6) at a concentration of 5 mM and 0.1% w/v sodium azide in D_2O at pH 7.0. The lower chloroform phase

constituted of nonpolar metabolites was collected to separate glass vials and the solvent was removed under a flow of nitrogen. The residue was then reconstituted using 600 µL deuterated chloroform (99.8 atom% D) containing 0.03% v/v TMS, after having recorded the yield.

^{1}H NMR Spectroscopy: An aliquot of 540 µL of the sample was transferred to a 5 mm NMR tube and the spectrum was recorded within 24 h of sample preparation using a 600 MHz Bruker Avance-III NMR spectrometer (Bruker BioSpin AG, Fällanden, Switzerland) equipped with a Prodigy TCI cryoprobe and a precooled SampleJet. A representative quality control sample obtained by pooling several samples was used in the optimization of acquisition parameters. Subsequently, the processes including sample loading, tuning and matching, acquisition, and processing were performed automatically by the ICONNMR platform from Bruker.

One-dimensional spectra were recorded using a noesygppr1d pulse sequence with 256 scans and 64K data points over a spectral width of 16 ppm, at a relaxation delay of 5 s, mixing time of 0.01 s, and an acquisition time of 3.40 s. Two-dimensional heteronuclear single quantum coherence (HSQC) and heteronuclear multiple bond coherence (HMBC) spectra were also recorded. The HSQC spectra were acquired using 32 scans, 1 k data points, 128 increments, 2 s relaxation delay, and spectral width of 16 and 165 ppm in the proton and carbon dimensions, respectively. The HMBC spectra were obtained using 64 scans, 1 k data points, 1.5 s relaxation delay, and 256 t1 increments at spectral widths of 13 and 220 ppm in the proton and carbon dimensions, respectively.

The preprocessing of the spectra such as phase and baseline correction was performed using Chenomx NMR Suite Professional 8.6 (Chenomx). The spectral region from 0 to 10 ppm was reduced to bins of size 0.04 (brain) and 0.02 (liver), based on the total area of the spectra using Chenomx NMR Suite after aligning the spectra using icoshift algorithm. The residual/baseline regions of the spectra without any peak as well as water (4.64–5.1 ppm) and methanol (3.4–3.5 ppm) were removed before normalization. The metabolite identities were established using the Chenomx Profiler module, adopting a peak-fitting approach. The quantification of metabolites was also achieved using the Chenomx Profiler module.

Multivariate and Univariate Statistical Analysis: The multivariate data generated by spectral binning was imported into SIMCA version 16.0.1 (Umetrics, Malmo, Sweden), and multivariate analysis tools such as PCA (Principal component analysis), PLS-DA (Partial least-squares discriminant analysis), and OPLS-DA (Orthogonal partial least squares-discriminant analysis) were applied. Considering every variable was equally important to the statistical results, prior to PCA the data were mean-centered and Pareto-scaled. Both PCA and OPLS models were constructed, and the number of components was determined by the standard seven-fold cross-validation method. The quality of multivariate analysis models was evaluated with R^2 values, indicating the explained variations, and Q^2 values, representing the model predictabilities, respectively. One (1) was the highest value of both parameters. Finally, the PLS-DA/OPLS-DA model significance was further assessed for robustness with the CV-ANOVA approach to ensure the statistical significance of the intergroup differentiations, with significance at $p < 0.05$.

For interpreting the multivariate classification models from OPLS-DA, the color-coded coefficient loading plot was used, enabling direct inspection and extraction of statistically significant and potentially biochemically important metabolites. The cut-off value of 0.7 (i.e., the critical value for the Pearson correlation coefficient) was chosen for the current study, and the discrimination significance of $p < 0.05$, played a critical role in extracting and identifying the statistically significant biomarkers.

All the results presented in this study were based on a three-step data analysis approach. First, PCA analysis was done to obtain unsupervised information about the group as well as metabolite differences between sample types. Secondly, PLS-DA and/or OPLS-DA were used as a supervised model to identify the significant biomarkers between different experimental groups. Thirdly, the statistical significances of the metabolites with a correlation coefficient value of ≥0.7 in the coefficient loading plot and a VIP value of ≥0.8 in the OPLS-DA were determined by univariate statistical analysis.

Univariate statistical analyses were performed using GraphPad Prism 8.0 (San Diego, USA) software. All data were reported as mean ± standard deviation (SD). The normal distribution of the data was tested using Shapiro–Wilk normality test. One-way analysis of variance (ANOVA) followed by Tukey's HSD with Bonferroni corrections was used to test the significance between the intervention groups if the data were normally distributed. Nonparametric Kruskal–Wallis test followed by Mann–Whitney *U* test was performed when the data were not normally distributed. The difference was regarded as statistically significant if the *p*-value was <0.05.

Supporting Information

Supporting Information is available from the Wiley Online Library or from the author.

Acknowledgements

This work was funded by the Research Council of Finland (Decision No.310982, Chiral lipids in chiral nature: a novel strategy for regio- and stereospecific research of human milk and omega-3 lipids; Decision No.356891, Structures and functions of chiral lipids: A stereospecific & multi-omics approach), and by the Finland-China Food and Health Network, as a strategic pilot programme of the Ministry of Education and Culture of Finland.

Conflict of Interest

The authors declare no conflict of interest.

Author Contributions

R.P.: Designing and execution of metabolomics study; analytical methods; investigations; data processing; writing-first draft; writing-reviewing and editing. Y.Z.: Design and execution of animal feeding trials, collection of organs and tissues; writing-reviewing and editing. G.H.: Synthesis of regio- and enantiopure triacylglycerols; writing-reviewing and editing. K.C.: Writing-reviewing and editing; K.L.: Designing animal feeding trials; writing-reviewing and editing. Y.B.: Conceptualization; designing animal feeding trial and metabolomics study; investigation; acquisition of funding and resources; project administration and supervision; writing-first draft; writing-reviewing and editing.

Data Availability Statement

The data that support the findings of this study are available from the corresponding author upon reasonable request.

Keywords

brain and liver, Docosahexaenoic acid, metabolomics, stearic acid, structured lipids

Received: May 25, 2023
Revised: December 30, 2023
Published online:

[1] R. K. Saini, Y. S. Keum, *Life Sci.* **2018**, *203*, 255.

[2] O. Kerdiles, S. Layé, F. Calon, *Trends Food Sci. Technol.* **2017**, *69*, 203.
[3] K. Gharami, M. Das, S. Das, *Neurochem. Int.* **2015**, *89*, 51.
[4] S. Vichi, L. Pizzale, L. S. Conte, *Eur. J. Lipid Sci. Technol.* **2007**, *109*, 72.
[5] H. Kallio, K. Yli-Jokipii, J. P. Kurvinen, O. Sjövall, R. Tahvonen, *J. Agric. Food Chem.* **2001**, *49*, 3363.
[6] M. S. Christensen, C. E. Høy, C. C. Becker, T. G. Redgrave, *Am. J. Clin. Nutr.* **1995**, *61*, 56.
[7] B. R. Na, J. H. Lee, *Molecules* **2020**, *25*, 5357.
[8] T. Karupaiah, K. Sundram, *Nutr. Metab. (Lond).* **2007**, *4*, 16.
[9] M. Kalpio, J. D. Magnússon, H. G. Gudmundsson, K. M. Linderborg, H. Kallio, G. G. Haraldsson, B. Yang, *Chem. Phys. Lipids* **2020**, *231*, 104937.
[10] S. W. Smith, *Toxicol. Sci.* **2009**, *110*, 4.
[11] K. M. Linderborg, A. Kulkarni, A. Zhao, J. Zhang, H. Kallio, J. D. Magnusson, G. G. Haraldsson, Y. Zhang, B. Yang, *Food Chem.* **2019**, *283*, 381.
[12] K. Tanaka, A. A. Farooqui, N. J. Siddiqi, A. S. Alhomida, W. Y. Ong, *Biomol. Ther. (Seoul).* **2012**, *20*, 152.
[13] P. C. Calder, *Proc. Nutr. Soc.* **2020**, *79*, 404.
[14] R. Valenzuela, M. Ortiz, M. C. Hernández-Rodas, F. Echeverría, L. A. Videla, *Curr. Med. Chem.* **2020**, *27*, 5250.
[15] M. Bélanger, I. Allaman, P. J. Magistretti, *Cell Metab.* **2011**, *14*, 724.
[16] D. Muñoz-Torrero, S. Rapposelli, M. Gütschow, M. J. Matos, M. Emília De Sousa, L. Saso, D. A. Butterfield, M. Favia, I. Spera, A. Campanella, M. Lanza, A. Castegna, *Mol.* **2022**, *27*, 951.
[17] K. M. Utzschneider, M. Kratz, C. J. Damman, M. Hullarg, *J. Clin. Endocrinol. Metab.* **2016**, *101*, 1445.
[18] C. Chudoba, K. Wardelmann, A. Kleinridders, *Biol. Chem.* **2019**, *400*, 991.
[19] F. Pifferi, S. C. Cunnane, P. Guesnet, *Nutrients* **2020**, *12*, 1382.
[20] P. Steiner, *Ann. Nutr. Metab.* **2019**, *75*, 8.
[21] D. Senyilmaz-Tiebe, D. H. Pfaff, S. Virtue, K. V. Schwarz, T. Fleming, S. Altamura, M. U. Muckenthaler, J. G. Okun, A. Vidal-Puig, P. Nawroth, A. A. Teleman, *Nat. Commun.* **2018**, *9*, 1.
[22] J. E. Sperringer, A. Addington, S. M. Hutson, *Neurochem. Res.* **2017**, *42*, 1697.
[23] C. Salcedo, J. V. Andersen, K. T. Vinten, L. H. Pinborg, H. S. Waagepetersen, K. K. Freude, B. I. Aldana, *Front Aging Neurosci.* **2021**, https://doi.org/10.3389/FNAGI.2021.736580.
[24] H. Ripps, W. Shen, *Mol. Vision* **2012**, *18*, 2673.
[25] M. Jakaria, S. Azam, M. E. Haque, S. H. Jo, M. S. Uddin, I. S. Kim, D. K. Choi, *Redox Biol.* **2019**, *24*, 101223.
[26] Z. Rafiee, A. M. García-Serrano, J. M. N. Duarte, *Nutr.* **2022**, *14*, 1292.
[27] Z. J. Wang, G. M. Li, B. M. Nie, Y. Lu, M. Yin, *Chem. Biol. Interact.* **2006**, *160*, 80.
[28] K. Govindpani, B. C. F. Guzmán, C. Vinnakota, H. J. Waldvogel, R. L. Faull, A. Kwakowsky, *Int. J. Mol. Sci.* **2017**, *18*, 1813.
[29] D. Cao, K. Kevala, J. Kim, H. S. Moon, S. B. Jun, D. Lovinger, H. Y. Kim, *J. Neurochem.* **2009**, *111*, 510.
[30] M. Hashimoto, S. Hossain, A. Al Mamun, K. Matsuzaki, H. Arai, *Crit. Rev. Biotechnol.* **2016**, *37*, 579.
[31] J. H. Liu, Q. Wang, Q. L. You, Z. L. Li, N. Y. Hu, Y. Wang, Z. L. Jin, S. J. Li, X. W. Li, J. M. Yang, X. H. Zhu, Y. F. Dai, J. P. Xu, X. C. Bai, T. M. Gao, *Nat. Commun.* **2020**, *11*, 1.
[32] R. J. S. Lacombe, R. Chouinard-Watkins, R. P. Bazinet, *Mol. Aspects Med.* **2018**, *64*, 109.
[33] D. Sugasini, R. Thomas, P. C. R. Yalagala, L. M. Tai, P. V. Subbaiah, *Sci. Rep.* **2017**, https://doi.org/10.1038/S41598-017-11766-0.
[34] R. K. McNamara, J. Able, R. Jandacek, T. Rider, P. Tso, D. M. Lindquist, *J. Lipid Res.* **2009**, *50*, 405.
[35] R. J. Lepping, R. A. Honea, L. E. Martin, K. Liao, I. Y. Choi, P. Lee, V. B. Papa, W. M. Brooks, D. J. Shaddy, S. E. Carlson, J. Colombo, K. M. Gustafson, *Dev. Psychobiol.* **2019**, *61*, 5.
[36] S. Yousf, D. M. Sardesai, A. B. Mathew, R. Khandelwal, J. D. Acharya, S. Sharma, J. Chugh, *Metabolomics* **2019**, https://doi.org/10.1007/S11306-019-1516-3.
[37] A. Kulkarni, A. Zhao, B. Yang, Y. Zhang, K. M. Linderborg, *Foods* **2022**, *11*, 208.
[38] J. A. T. Wood, J. S. Williams, L. Pandarinathan, D. R. Janero, C. J. Lammi-Keefe, A. Makriyannis, *J. Lipid Res.* **2010**, *51*, 1416.
[39] S. I. Rapoport, J. S. Rao, M. Igarashi, *Prostaglandins. Leukot. Essent. Fatty Acids* **2007**, *77*, 251.
[40] S. C. Dyall, *Front. Aging Neurosci.* **2015**, *7*, 52.
[41] K. M. Linderborg, H. P. T. Kallio, *Food Rev. Int.* **2007**, *21*, 331.
[42] H. Mu, T. Porsgaard, *Prog. Lipid Res.* **2005**, *44*, 430.
[43] T. Kühn, A. Floegel, D. Sookthai, T. Johnson, U. Rolle-Kampczyk, W. Otto, M. von Bergen, H. Boeing, R. Kaaks, *BMC Med.* **2016**, *14*, 13.
[44] P. M. Kris-Etherton, A. E. Griel, T. L. Psota, S. K. Gebauer, J. Zhang, T. D. Etherton, *Lipids* **2005**, *40*, 1193.
[45] B. Kristinsson, K. M. Linderborg, H. Kallio, G. G. Haraldsson, *Tetrahedron: Asymm.* **2014**, *25*, 125.
[46] S. Ghasemifard, G. M. Turchini, A. J. Sinclair, *Prog. Lipid Res.* **2014**, *56*, 92.
[47] G. Kaur, D. P. Begg, D. Barr, M. Garg, D. Cameron-Smith, A. J. Sinclair, *Br. J. Nutr.* **2010**, *103*, 32.
[48] S. Reagan-Shaw, M. Nihal, N. Ahmad, *FASEB J.* **2007**, *22*, 659.
[49] O. Beckonert, H. C. Keun, T. M. D. Ebbels, J. Bundy, E. Holmes, J. C. Lindon, J. K. Nicholson, *Nat. Protoc.* **2007**, *2*, 2692.